

# Non-Abelian gauge potential driven localization transition in quasiperiodic optical lattices

En Guo Guan, Hang Yu, and Gang Wang\*

*School of Physical Science and Technology, Soochow University, Suzhou 215006, China*

Gauge potential is an emergent concept in systems of ultracold atomic gases. Derived from quantum waves immersed in an *Abelian* gauge, the quasiperiodic Aubry-Andre-Harper (AAH) model is a simple yet powerful Hamiltonian to study the Anderson localization of ultracold atoms. In this work, we investigate the localization properties of ultracold atoms trapped in quasiperiodic optical lattices subject to a non-Abelian gauge, which can be depicted by a family of non-Abelian AAH models. We identify that the non-Abelian AAH models can bear the self-duality under the Fourier transformation. We thus analyze the localization transition of this self-dual non-Abelian quasiperiodic optical lattices, revealing that the non-Abelian gauge involved drives a transition from a pure delocalization phase, then to coexistence phases, and then finally to a pure localization phase. This is in stark contrast to the Abelian AAH model that does not support the coexistence phases. Our results thus comprise a new insight on the fundamental aspects of Anderson localization in quasiperiodic systems, from the perspective of non-Abelian gauge.

arXiv:1908.06839v1 [cond-mat.quant-gas] 19 Aug 2019

---

\* [phwanggang@gmail.com](mailto:phwanggang@gmail.com)

## I. INTRODUCTION

A magnetic field, through its geometric gauge potential, usually causes measurable effects on the wave functions. This concept of gauge potential has been fueling research since Aharonov and Bohm's seminal work [1]. In particular, the recent explorations of gauge fields synthesized for neutral atoms open up many avenues in the field of ultracold atomic gases [2–8]. Among them the synthetic non-Abelian gauge in the atomic gases with internal degrees of freedom is of special interest because of the high gauge symmetry. The non-Abelian gauge will emerge in cold-atom systems when the orbital motion is coupled to the internal hyperfine levels. Therefore, the non-Abelian gauge is usually responsible for various (pseudo)spin-orbit interactions in the ultracold atoms. In this case, the Aharonov-Bohm phase will be replaced by a matrix that can bear its imprint on the different internal states [9].

In parallel to the synthetic gauge potentials, another timely topic in the ultracold atoms is the Anderson localization, where researchers try to understand the intricate effects of disorder. The effect of disorder originates from the interference of multiple scattering paths in the disordered configurations. Therefore, strong enough disorder could bring about the destructive interference, so that arrest transport completely, leading to a phase transition from delocalized (“metal” phase) to exponentially localized (“insulator” phase) states [10–14]. The concept of Anderson localization has been progressively developed from its original scope of solid-state physics to the context of ultracold atomic gases, in which a vast number of model Hamiltonians can be realized by engineering appropriate optical potentials [15]. Within this setting, a range of fascinating localization phenomena has been revealed successfully, including the direct observations of weak localization [16, 17], the Anderson localization in 1D [18, 19] and 3D systems [20, 21], and mobility edges [22], just to mention a few.

Concerning the Anderson localization of ultracold atoms, quasiperiodic optical lattices arouse a recent surge of interest [19]. Aubry and André have analytically demonstrated that the one-dimensional lattice with a quasiperiodic modulation, the so-called Aubry-André-Harper (AAH) model [23, 24], can show the localization transition. One of the key features of the AAH model is either *all* states being extended or localized, depending on the modulation strength of the quasiperiodic potential. This localization transition in the space of modulation strength arises from the self-duality of the AAH model. As a result, either ballistic or localized excitations were observed in the AAH optical lattices [19]. Distinct from the truly random disorder, the disorder for the quasiperiodic lattice is introduced in a deterministic manner. Even so, the coexistence phase, defined as the regime in which the localized and extended states exist simultaneously under the same disorder strength, can appear in 1D quasiperiodic models [25–35], as is the case for the higher-dimensional disordered models with true randomness. The coexistence phase has been experimentally observed in the quasiperiodic optical lattices [36, 37].

Motivated by the ongoing progress in synthetic gauge potential and Anderson localization using ultracold atoms, several natural while interesting questions arise, from the point of view of the non-Abelian gauge: Under the presence the non-Abelian gauge is it possible to construct a family of self-dual models? If that, what is the localization property of such self-dual non-Abelian lattices? And what is the associated phase diagram?

In the current work we answer these questions through studying the cold atoms trapped in quasiperiodic optical lattices which are subject to non-Abelian  $SU(2)$  gauge potentials. The optical lattices can be modeled by a family of non-Abelian AAH Hamiltonians. We show that the non-Abelian gauge has dramatic consequences on the localization of ultracold atoms in quasiperiodic optical lattices. To be specific, such non-Abelian quasiperiodic lattices become self-dual under the Fourier transformation, whereas the coexistence phase composed of localized and extended states can emerge, manifesting itself as definite mobility edges in the energy space. We present evidence that supports these observations by employing two kind of measures of localization designed to treat the quasiperiodic lattices, inclusive of inverse participation ratio and the decomposition of spectrum. Comparing to its Abelian counterpart, we reveal a rich phase diagram driven by the non-Abelian gauge, featuring a transition of metal-coexistence I-coexistence II-Anderson insulator. This is in marked contrast with the Abelian AAH model, therein being self-dual while having no coexistence phase.

The paper is organized as follows. In Sec. II, we firstly review the results of Anderson localization in 1D quasiperiodic Abelian AAH model, which will be useful in the following. Then, we formulate the non-Abelian optical lattices with quasiperiodic modulations in Sec. III, and analyze the relevant localization properties. We finally summarize our results in Sec. IV. Hereafter, the non-Abelian AAH model will be referred to as the NA-AAH model so as to distinguish it from its Abelian counterpart, i.e., the original AAH model (abbreviated as A-AAH model).

## II. SHORT REVIEW OF QUASIPERIODIC A-AAH HAMILTONIAN

Before elaborating on our results, it will be instructive to make some general reviews on the localization properties of the standard quasiperiodic A-AAH lattice [23]. The parent model for the one-dimensional A-AAH lattice is the Hofstadter Hamiltonian, depicting the electrons hopping in the square lattice threaded by a homogeneous magnetic

field corresponding to an *Abelian*  $U(1)$  gauge potential. The Hofstadter Hamiltonian reads

$$\mathcal{H} = - \sum_{m,n} J_x \psi_{m+1,n}^\dagger \psi_{m,n} + J_y \psi_{m,n+1}^\dagger e^{i\theta_y} \psi_{m,n} + h.c. \quad (1)$$

under the Landau gauge [38]. Here  $\psi_{m,n}^\dagger, \psi_{m,n}$  are the creation and annihilation operators on the lattice site ( $x = m, y = n$ ), the phase factors are given by  $\theta_y = 2\pi\Omega m$  where  $\Omega$  is the magnetic flux  $\Phi$  in units of the flux quantum  $\Phi_0$  penetrating each plaquette,  $J_{x,y}$  represents the nearest-neighbor hopping amplitudes. In a mixed momentum-position space as obtained by performing the Fourier transformation only along the  $y$  direction, Eq. 1 reduces to the celebrated A-AAH Hamiltonian [23]

$$\mathcal{H} = - \sum_m \psi_{m+1}^\dagger \psi_m + \psi_{m-1}^\dagger \psi_m + 2\lambda \cos(2\pi\Omega m + k_y) \psi_m^\dagger \psi_m, \quad (2)$$

where  $\lambda$  parametrizes the ratio  $J_y/J_x$  and denotes the modulation strength of the potential. An irrational  $\Omega$  (usually the golden mean) ensures the quasiperiodic lattices. Without loss of generality, we assume  $k_y = 0$  below. One premier feature of the quasiperiodic A-AAH model is its self-duality: Upon Fourier transformation, which exchanges the real and momentum space, Eq. (2) can be proven to be dual to itself, with  $\lambda \rightarrow \lambda^{-1}$ . Exactly at  $\lambda = 1$  the model is invariant under the duality, identified as the transition point to separate the pure localization and pure delocalization phases. Therefore, for  $\lambda < 1$  all the states are delocalized, while  $\lambda > 1$  makes all of the states exponentially localized. This model shows the localization-delocalization transition without the presence of the energy-dependent mobility edges in the phase diagram. Such a transition has been observed experimentally in a noninteracting bosonic gas [19]. On the other hand, there are variations that enrich the localization transition [25–37], e.g., the emergence of mobility edges in the 1-dimensional quasiperiodic systems as that in 3-dimensional space of truly random disorder.

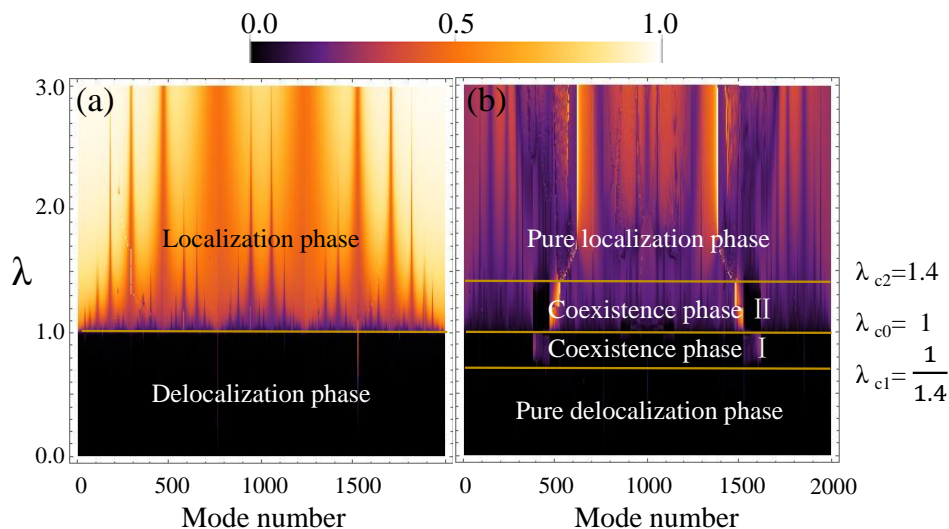


FIG. 1. (Color online) The IPR distribution of states as a function of  $\lambda$ . (a) A-AAH model, (b) NA-AAH model with a fixed non-Abelian strength  $q = 0.3\pi$ . The states are sorted in descending order according to their energies. The lines are indicative of the critical modulation strengths to separate various phases, and the relevant values are estimated through spectral measures elaborated below in subsec. III B.

To quantify the localization properties of the wave functions, we calculate the inverse participation ratio (IPR) of states defined as follows [13]:

$$\text{IPR}^{(i)} = \frac{\sum_m |\psi_m^{(i)}|^4}{(\sum_m |\psi_m^{(i)}|^2)^2}, \quad (3)$$

where the superscript  $i$  denotes the  $i$ th state  $\psi^{(i)}$ . For a spatially extended state, the IPR approaches zero whereas it is finite for a localized state. Therefore, the IPR can be taken as a criterion to distinguish the extended states from the localized ones [13]. Figure 1 (a) illustrates clear distinctions of IPRs for various modulation strength. Obviously this indicates that a sharp localization-delocalization transition occurs in the quasiperiodic A-AAH model at the dual point  $\lambda = 1$ , beyond which *all* states convert from extended to localized.

### III. ANDERSON LOCALIZATION IN QUASIPERIODIC NA-AAH OPTICAL LATTICES

#### A. NA-AAH Hamiltonian and its self-duality

The gauge field used in the original AAH model is of the Abelian type. Quite recently, there are proposals to generate non-Abelian gauge fields in optical lattices [4, 5]. Now we turn to the quasiperiodic non-Abelian AAH model, which originates from the Hofstadter Hamiltonian in a non-Abelian optical lattice [39], and investigate its localization properties.

Our starting point is the two-component cold atoms characterized by two internal degrees of freedom, providing a (pseudo)spinor  $\Psi = (\psi^\dagger, \psi^\downarrow)^T$ . The ultracold gases are trapped in a 2-dimensional optical square lattice. We impose a synthetic non-Abelian gauge potential on the optical lattice

$$\mathbf{A} = (q\sigma_y, 2\pi\Omega m\sigma_0 + q\sigma_x, 0). \quad (4)$$

Here  $\sigma_{x(y)}$  denotes the Pauli operator. The gauge field  $\mathbf{A}$  is constituted by an Abelian U(1) term  $\mathbf{A}_a = (0, 2\pi\Omega m\sigma_0, 0)$ , and by a constant SU(2) term  $\mathbf{A}_{na} = q(\sigma_y, \sigma_x, 0)$  proportional to the parameter  $q$ , quantifying the strength of the non-Abelian gauge. This gauge potential may be generated using a two dimensional optical superlattice based on laser-assisted spin-dependent hopping [4, 5, 39–42]. The non-Abelian gauge flux  $q$  is determined by the Rabi frequencies of the two-photon off-resonant transition and can be tuned via changing the laser field intensity. The SU(2) non-Abelian part is the new ingredient as compared with the original Hofstadter Hamiltonian (Eq. 1). According to the Peierls substitution, the non-Abelian component imprints an internal-state-dependent phase factor on the hoppings, and changes the internal states of the spinor. The corresponding non-Abelian Hofstadter Hamiltonian reads [39]

$$H = - \sum_{m,n} \Psi_{m+1,n}^\dagger J_x e^{iq\sigma_y} \Psi_{m,n} + \Psi_{m,n+1}^\dagger J_y e^{i(q\sigma_x + 2\pi\Omega m)} \Psi_{m,n} + h.c.. \quad (5)$$

By taking periodic and open boundary conditions along  $y$  and  $x$  directions separately, the Hamiltonian will be transformed into

$$\begin{aligned} \mathcal{H} = & - \sum_m 2\lambda \Psi_m^\dagger \begin{pmatrix} \cos q \cos(2\pi\Omega m) & -\sin q \sin(2\pi\Omega m) \\ -\sin q \sin(2\pi\Omega m) & \cos q \cos(2\pi\Omega m) \end{pmatrix} \Psi_m \\ & + \Psi_{m+1}^\dagger \begin{pmatrix} \cos q & \sin q \\ -\sin q & \cos q \end{pmatrix} \Psi_m + \Psi_{m-1}^\dagger \begin{pmatrix} \cos q & -\sin q \\ \sin q & \cos q \end{pmatrix} \Psi_m. \end{aligned} \quad (6)$$

Compared with Eq. 2, the Hamiltonian Eq. 6 involves a non-Abelian gauge. Thus we name it non-Abelian AAH model.

The Fourier transformation of Eq. 6 provides the following equation in the dual space:

$$\begin{aligned} \mathcal{H}^* = & - \sum_k 2\Psi_k^\dagger \begin{pmatrix} \cos q \cos(2\pi\Omega k) & -\sin q \sin(2\pi\Omega k) \\ -\sin q \sin(2\pi\Omega k) & \cos q \cos(2\pi\Omega k) \end{pmatrix} \Psi_k \\ & + \lambda \Psi_{k+1}^\dagger \begin{pmatrix} \cos q & \sin q \\ -\sin q & \cos q \end{pmatrix} \Psi_k + \lambda \Psi_{k-1}^\dagger \begin{pmatrix} \cos q & -\sin q \\ \sin q & \cos q \end{pmatrix} \Psi_k. \end{aligned} \quad (7)$$

Definitely, Eq. 7 takes the same form as that in real space (Eq. 6) with just the coefficients being interchanged. Hence the NA-AAH model embodies the self-duality, ensuring that a state which is extended in the parameter space  $(\lambda, q)$  will be converted into a localized state in  $(\frac{1}{\lambda}, q)$ , and vice versa. As a result,  $\lambda_{c0} = 1$  is identified as a transition point.

#### B. localization properties

Having described the self-duality of the NA-AAH optical lattices, we now turn to the localization properties, and show the nontrivial effect stemming from the non-Abelian gauge. In order to assess the localization properties, we first perform the numerical calculations of the IPRs, which is shown in Fig. 1(b).

Obviously, the IPR diagram in Fig. 1 (b) provides four regimes separated by  $\lambda_{c1}$ ,  $\lambda_{c2}$ , and  $\lambda_{c0}$ , *i.e.*, pure delocalization phase, coexistence phase I, and coexistence phase II, and pure localization phase. When the modulation strength  $\lambda$  is sufficiently small ( $< \lambda_{c1}$ ), IPR values are approximately vanishing for all states, indicating that all

states are extended and the cold atoms are in the pure delocalization phase. Coexistence phases emerge within the regime from  $\lambda_{c1}$  to  $\lambda_{c2}$ . The term ‘‘coexistence’’ herein denotes that the localized and extended states can be found at the same disorder strength, while they are separated by critical energies called mobility edges. The two coexistence phases, labeled by I and II, are separated by the self-dual point  $\lambda_{c0} = 1$ . As  $\lambda$  is increased further ( $> \lambda_{c2}$ ) the non-Abelian system enters into the pure localization phase and all states are found to be localized, illustrated by the near-unity IPRs. Apparently, this diagram is qualitatively different from the A-AAH model, wherein only two phases of pure delocalization and localization are supported. The unique coexistence phases arise from the introduction of non-Abelian gauge.

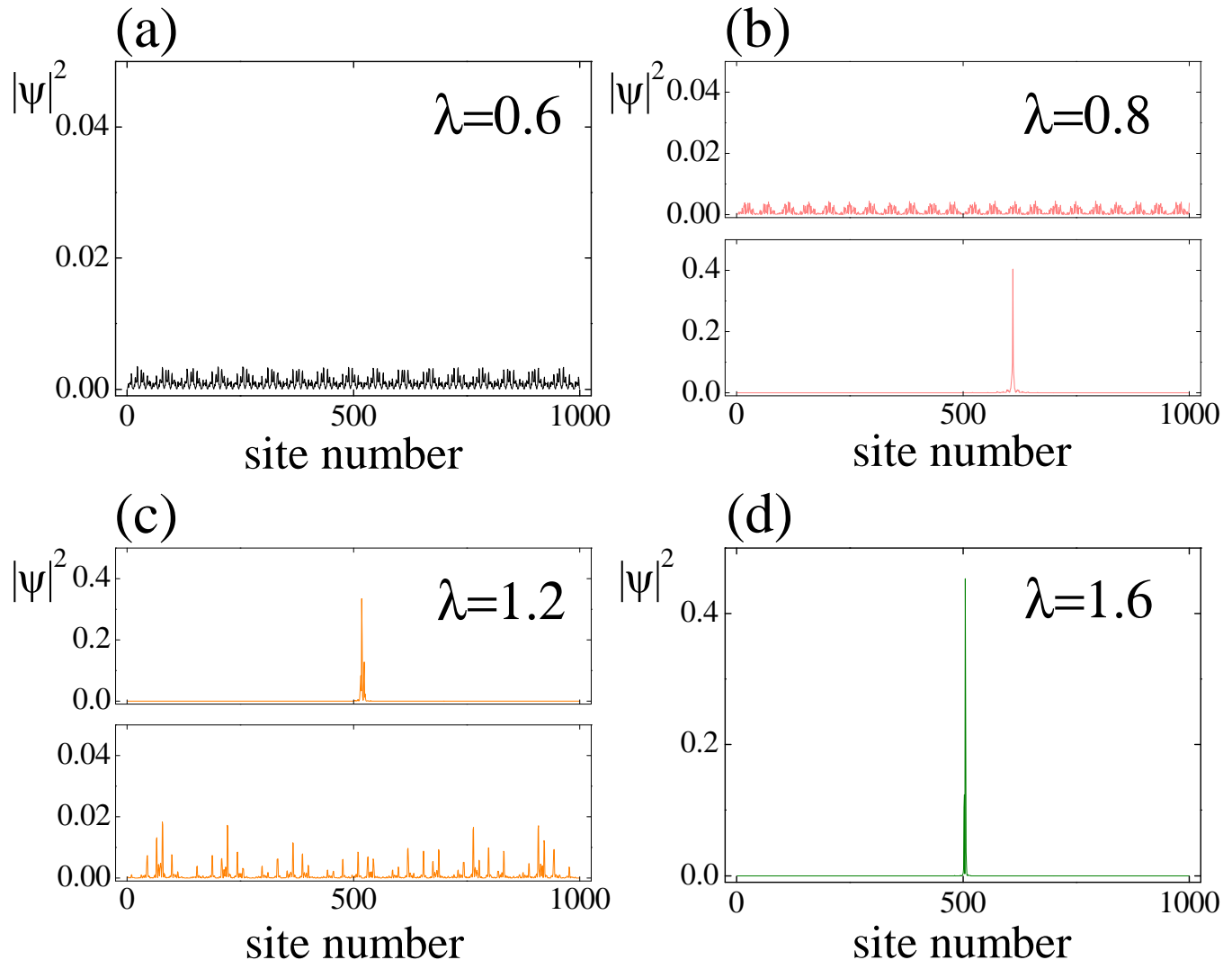


FIG. 2. (Color online) For a fixed non-Abelian gauge component  $q = 0.3\pi$ , corresponding to Fig. 1 (b), the typical states in various localization regimes, i.e.,  $\lambda = 0.6$  (a),  $\lambda = 0.8$  (b),  $\lambda = 1.2$  (c),  $\lambda = 1.6$  (d).

To favor that the distinctions of IPRs do guarantee various phases, we summarize in Fig. 2 the typical states at various  $\lambda$ 's. In the purely delocalized regime, all the states extend over the entire system [Fig. 2(a)]. In the coexistence phase I, the extended and exponentially localized states present simultaneously for the same modulation [Fig. 2(b)]. In the coexistence phase II ( $\lambda_{c2} > \lambda > \lambda_{c0}$ ) the spatial behavior is similar to that of phase I [Fig. 2(c)]. At the strength  $\lambda > \lambda_{c2}$ , all the states become spatially localized, as shown in Fig. 2(d).

In order to further corroborate our findings on the appearance of coexistence phases in the quasiperiodic non-Abelian optical lattices (that is so far based on IPR analysis of finite size systems), we now implement the spectral analysis to identify the phase diagram. The decomposition of energy spectrum is intimately related to the localization property of the corresponding system [43, 44]. Specifically, an absolutely continuous spectrum corresponds to a delocalization phase. While a pure point spectrum is associated with the purely localized regime as in randomly disordered systems.

Finally, there is a critical regime at the metal insulator transition, where the spectrum becomes singular continuous. Thereby, we can resort to the total width of allowed energy bands to diagnose various phases.

Note that the quasiperiodic optical lattice is a non-periodic structure, and therefore it is not possible to access the band spectrum directly. Hence, we approximate the irrational number  $\Omega = (\sqrt{5} - 1)/2$  by the ratio of two successive Fibonacci terms  $\Omega' = F_{l-1}/F_l$ , where the Fibonacci sequence is defined by the recurrence relation  $F_l = F_{l-1} + F_{l-2}$ . As  $l$  increases the rational number  $\Omega'$  converges to the golden ratio. Within this approximation the quasiperiodic model reduces to a periodic superlattice which has a unit cell of length  $F_l$ . Thereby, as  $l \rightarrow \infty$  the spectrum of the periodic superlattices asymptotically approaches that of quasiperiodic case and consequently the band width of quasiperiodic lattices can be accessed. Via its spectral measures, we can define the decomposition of the spectrum of the NA-AAH quasiperiodic optical lattices, and further identify the phase diagram.

We first test our method by monitoring the development of the total band width  $\mathcal{W}_r(\lambda, q)$  of the real-space Hamiltonian (Eq. 6) with the increase of the superlattice period, *viz.* Fibonacci terms  $F_l$ , for a given modulation strength  $\lambda$  and non-Abelian gauge  $q$ . As shown in Fig. 3, the band widths exhibit a falling-off, accompanied by various tendencies dependent on the modulation strengths. For the weak modulations ( $\lambda = 0.6, 0.8$ ),  $\mathcal{W}_r$  will converge to a finite value as one follows the Fibonacci sequence. The  $\lambda = 1.2$  curve also presents the similar behavior. This shows the existence of extended states for these modulations. On the other hand, an algebraic decay  $\mathcal{W}_r \propto F_l^{-\delta}$  emerges at  $\lambda = 1$  (solid circles in Fig. 3), demonstrating that this is Cantor spectrum and a transition occurs [43]. At the stronger modulation ( $\lambda = 1.6$ ), by contrast,  $\mathcal{W}_r$  shrinks to zero *exponentially*, signaling a point spectrum attained. This vanishing asymptotic value ( $\mathcal{W}_r \approx 0$ ) directly marks the regime of pure localization of the NA-AAH quasiperiodic lattice. These results are in agreement with the IPR analysis aforementioned.

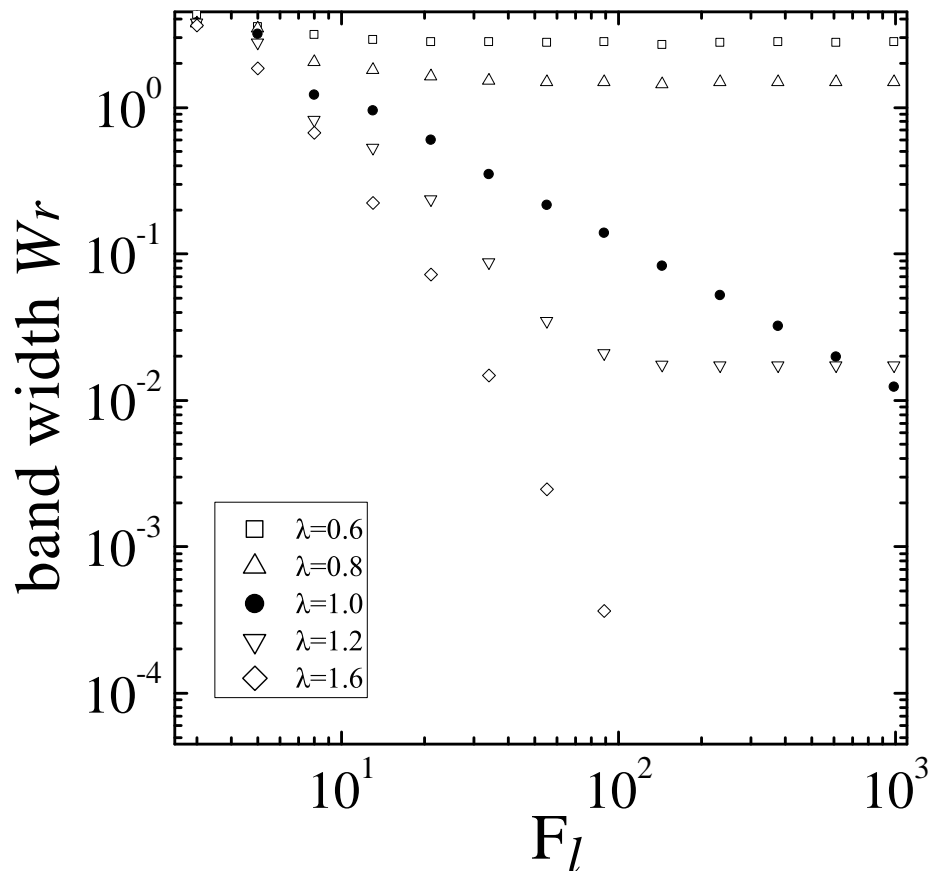


FIG. 3. (Color online) (a) Total width  $\mathcal{W}_r$  of allowed energy bands versus the period of the NA-AAH lattice, being equal Fibonacci number  $F_l$ . The limit  $F_l \rightarrow \infty$  represents the quasiperiodic system. All data points are with a fixed non-Abelian gauge component  $q = 0.3\pi$ . Please note the double logarithmic plot.

Importantly, it should be noted that  $\mathcal{W}_r$  alone is inadequate to distinguish the coexistence phases from the pure delocalization phases. This is ascribed to the fact that the finiteness of  $\mathcal{W}_r$  is insensitive to the mixing of the point spectrum (associated with the localized states) inside the continuous spectrum (associated with the extended states).

Hence, another metric we use is the band width in dual space, *i.e.*, the band-width  $\mathcal{W}^*$  of Hamiltonian 7. This quantity quantizes the decomposition of the energy spectrum in dual space. Note that the two quantities  $\mathcal{W}_r$  and  $\mathcal{W}^*$  are complementary in discerning the localization phases, given the self-duality between Hamiltonians 6 and 7. Thereby, the simultaneous measures of both quantities can serve as an order parameter of the phase diagram. To be specific, the presence of the pure metal phase is characterized by the finite  $\mathcal{W}_r$  and the vanishing  $\mathcal{W}^*$ , whereas the pure localization phase is indicated by the zero  $\mathcal{W}_r$  and the finite  $\mathcal{W}^*$ . In between, a coexistence regime is found when both indices are simultaneously finite. Therefore, the combination of  $\mathcal{W}_r$  and  $\mathcal{W}^*$  will provide unambiguous evidence for distinct phases.

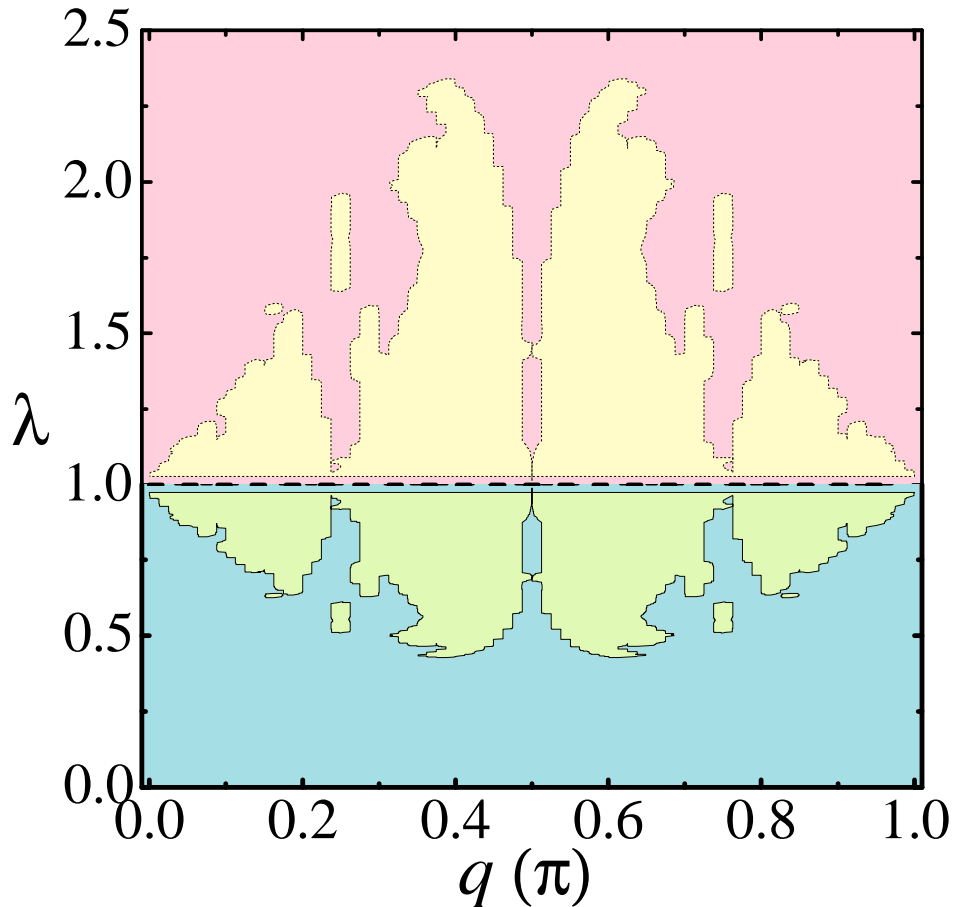


FIG. 4. (Color online) Localization phase diagram of the quasiperiodic NA-AAH lattice obtained from the band width data  $\mathcal{W}_r$  and  $\mathcal{W}^*$ . Solid lines are the separatrices to divide different regions, which are extracted through the vanishing values of  $\mathcal{W}_r$  and  $\mathcal{W}^*$ . Due to the computational accuracy we take  $1.0 \times 10^{-7}$ . Clearly four regions are observed. The blue-shaded region is characterized by  $\mathcal{W}_r > 1.0 \times 10^{-7}$  and  $\mathcal{W}^* < 1.0 \times 10^{-7}$ . In the yellow-shaded region both  $\mathcal{W}_r$  and  $\mathcal{W}^*$  are simultaneously larger than  $1.0 \times 10^{-7}$ . This area is further separated into two parts by the self-dual line  $\lambda_{c0} = 1$  (dashed line). The red-shaded region is with  $\mathcal{W}_r < 1.0 \times 10^{-7}$  and  $\mathcal{W}^* > 1.0 \times 10^{-7}$ .

Based on these arguments, we scan the band width data to extract the separatrices among different phases in  $\lambda - q$  plane. As seen from Fig. 4, we find that for a non-Abelian gauge  $q$ , the quasiperiodic NA-AAH lattice passes through four phases, including the pure delocalization-coexistence I-coexistence II-pure localization, as  $\lambda$  increases. In the blue-shaded area, we always find a finite value of  $\mathcal{W}_r$  ( $\mathcal{W}_r > 0$ ) whereas a vanishing  $\mathcal{W}^*$  ( $\mathcal{W}^* \approx 0$ ). This characterizes the absence of any localized state, namely the pure delocalization regime. In the red-shaded area, we find a fully localized phase, which is marked by  $\mathcal{W}_r \approx 0$  while  $\mathcal{W}^* > 0$ . This is the pure localization regime. In between, an intermediate regime (yellow-shaded area) is found where  $\mathcal{W}_r > 0$  and  $\mathcal{W}^* > 0$ . This directly illustrates the cooccurrence of extended and localized states in this area, in which mobility edges are present. Furthermore, the coexistence phase is split into two distinct regions I and II by the self-dual point  $\lambda_{c0} = 1$ . It is worth noting that for  $q = 0, \pi/2$ , and  $\pi$  the coexistence phases essentially disappear. In other words, the localization transition is similar to that of Abelian AAH lattices. The reason lies on the fact that the NA-AAH lattice with  $q = 0, \pi$  can be mapped

accurately onto two decoupled Abelian replicas which have no mobility edges individually. And  $q = \pi/2$  reduces Eq. 5 to the Abelian flux model [39]. Moreover, we find the reentrant coexistence phases appears far away from the self-dual line, as indicated by the circled areas in the pure delocalization (localization) phase. Interestingly, we notice that Fig. 4 embodies beautiful symmetries. Firstly, the localization phase diagram is symmetric with respect to the axis  $q = \pi/2$ . We also find the reflection symmetry about  $\lambda = 1$ , inversely scaled by  $1/\lambda$ . This  $\lambda \leftrightarrow \frac{1}{\lambda}$  symmetry results from the self-duality of the NA-AAH Hamiltonian.

#### IV. DISCUSSION AND CONCLUSION

Before concluding we should point that the ultracold atoms studied here are immersed in a non-Abelian gauge. These are not the non-Abelian particles respecting the non-Abelian exchange statistics. Therefore, our work differs fundamentally from the previous work [45]. Therein are the localization of  $p$ -wave. On the other hand, there has been one work proposed a quasiperiodic lattices with non-Abelian gauge [46]. However, the non-Abelian gauge used there is characterized by the spatial inhomogeneity, and the Hamiltonian has not yet been determined to be self-dual.

In conclusion, we have combined two vital concepts, disorder and non-Abelian gauge, and unveiled rich localization phases of cold atoms in the non-Abelian quasiperiodic optical lattices. Besides the pure metal and pure insulator, we found the emergent coexistence phases. In other words, for a quasiperiodic optical lattice, the non-Abelian gauge can drive a localization transition in an engineered manner. This represents the high sensitivity of global transport of ultracold atoms to the non-Abelian configurations. Therefore, our results are fundamentally different from the extensively studied Abelian quasiperiodic problems. We also developed a method to identify the localization phase diagram: diagnosing the decomposition of the energy spectra in both real and dual spaces. This method is accurate and general. In a word, the marriage of Anderson localization and non-Abelian gauge potential may open up exciting new physics and could enrich our understanding of the metal-insulator transition.

#### ACKNOWLEDGMENTS

The authors are indebted to Prof. Ray Kuang Lee from National Tsing Hua University for stimulating discussions. This work is supported by the National Natural Science Foundation of China (11604231); Natural Science Foundation of Jiangsu Province under Grant (BK20160303); Natural Science Foundation of the Jiangsu Higher Education Institutions of China (16KJB140012); Priority Academic Program Development (PAPD) of Jiangsu Higher Education Institutions.

- 
- [1] Y. Aharonov and D. Bohm, “Significance of electromagnetic potentials in the quantum theory,” *Phys. Rev.* **115**, 485 (1959).
  - [2] V. Galitski, Ian Spielman, and G. Juzeliūnas, “Artificial Gauge Fields with Ultracold Atoms,” *Physics Today* **72**, 39 (2019).
  - [3] D. Jaksch and P. Zoller, “Creation of effective magnetic fields in optical lattices: the Hofstadter butterfly for cold neutral atoms,” *New J. Phys.* **5**, 56 (2003).
  - [4] K. Osterloh, M. Baig, L. Santos, P. Zoller, and M. Lewenstein, “Cold Atoms in Non-Abelian Gauge Potentials: From the Hofstadter Moth to Lattice Gauge,” *Phys. Rev. Lett.* **95**, 010403 (2005).
  - [5] J. Ruseckas, G. Juzeliūnas, P. Öhberg, and M. Fleischhauer, “Non-Abelian Gauge Potentials for Ultracold Atoms with Degenerate Dark States,” *Phys. Rev. Lett.* **95**, 010404 (2005).
  - [6] Jean Dalibard, Fabrice Gerbier, Gediminas Juzeliūnas, and Patrik Öhberg, “Artificial gauge potentials for neutral atoms,” *Rev. Mod. Phys.* **83**, 1523 (2011).
  - [7] N. Goldman, G. Juzeliūnas, P. Öhberg, I. B. Spielman, “Light-induced gauge fields for ultracold atoms,” *Rep. Prog. Phys.* **77**, 126401 (2014).
  - [8] M. Aidelsburger, S. Nascimbene, and N. Goldman, “Artificial gauge fields in materials and engineered systems,” *C. R. Phys.* **19**, 394 (2018).
  - [9] F. Wilczek and A. Zee, “Appearance of Gauge Structure in Simple Dynamical Systems,” *Phys. Rev. Lett.* **52**, 2111 (1984).
  - [10] P. W. Anderson, “Absence of Diffusion in Certain Random Lattices,” *Phys. Rev.* **109**, 1492 (1958).
  - [11] E. Abrahams, P. W. Anderson, D. C. Licciardello, and T. V. Ramakrishnan, “Scaling Theory of Localization: Absence of Quantum Diffusion in Two Dimensions,” *Phys. Rev. Lett.* **42**, 673 (1979).
  - [12] P. A. Lee and T. V. Ramakrishnan, “Disordered electronic systems,” *Rev. Mod. Phys.* **57**, 287 (1985).
  - [13] B. Kramer and A. MacKinnon, “Localization theory and experiment,” *Rep. Prog. Phys.* **56**, 1469 (1993).
  - [14] F. Evers and A. D. Mirlin, “Anderson transitions,” *Rev. Mod. Phys.* **80**, 1355 (2008).
  - [15] I. Bloch, J. Dalibard, and W. Zwerger, “Many-body physics with ultracold gases,” *Rev. Mod. Phys.* **80**, 885 (2008).

- [16] F. Jendrzejewski *et al.*, “Coherent Backscattering of Ultracold Atoms,” *Phys. Rev. Lett.* **109**, 195302 (2012).
- [17] K. Müller *et al.*, “Suppression and Revival of Weak Localization through Control of Time-Reversal Symmetry,” *Phys. Rev. Lett.* **114**, 205301 (2015).
- [18] J. Billy *et al.*, “Direct observation of Anderson localization of matter waves in a controlled disorder,” *Nature* **453**, 891 (2008).
- [19] G. Roati *et al.*, “Anderson localization of a non-interacting Bose Einstein condensate,” *Nature* **453**, 895 (2008).
- [20] S. S. Kondov, W. R. McGehee, J. J. Zirbel, and B. DeMarco, “Three-Dimensional Anderson Localization of Ultracold Matter,” *Science* **334**, 66 (2011).
- [21] F. Jendrzejewski *et al.*, “Three-dimensional localization of ultracold atoms in an optical disordered potential,” *Nature Phys.* **8**, 398 (2012).
- [22] G. Semeghini *et al.*, “Measurement of the mobility edge for 3D Anderson localization,” *Nat. Phys.* **11**, 554 (2015).
- [23] S. Aubry and G. André, “Analyticity breaking and Anderson localization in incommensurate lattices,” *Ann. Isr. Phys. Soc.* **3**, 133 (1980).
- [24] P. G. Harper, “Single Band Motion of Conduction Electrons in a Uniform Magnetic Field,” *Proc. Phys. Soc. A* **68**, 874 (1955).
- [25] S. Das Sarma, S. He, and X. C. Xie, “Mobility Edge in a Model One-Dimensional Potential,” *Phys. Rev. Lett.* **61**, 2144 (1988).
- [26] D. J. Thouless, “Localization by a Potential with Slowly Varying Period,” *Phys. Rev. Lett.* **61**, 2141 (1988).
- [27] Dave J. Boers, Benjamin Goedeke, Dennis Hinrichs, and Martin Holthaus, “Mobility edges in bichromatic optical lattices,” *Phys. Rev. A* **75**, 063404 (2007).
- [28] J. Biddle and S. Das Sarma, “Predicted Mobility Edges in One-Dimensional Incommensurate Optical Lattices: An Exactly Solvable Model of Anderson Localization,” *Phys. Rev. Lett.* **104**, 070601 (2010).
- [29] S. Ganeshan, J. H. Pixley, and S. Das Sarma, “Nearest Neighbor Tight Binding Models with an Exact Mobility Edge in One Dimension,” *Phys. Rev. Lett.* **114**, 146601 (2015).
- [30] M. L. Sun, G. Wang, N. B. Li, and T. Nakayama, “Localization-delocalization transition in self-dual quasiperiodic lattices,” *Europhys. Lett.* **110**, 57003 (2015).
- [31] M. Johansson and R. Riklund, “Self-dual model for one dimensional incommensurate crystals including next-nearest-neighbor hopping, and its relation to the Hofstadter model,” *Phys. Rev. B* **43**, 13468 (1991).
- [32] S. Gopalakrishnan, “Self-dual quasiperiodic systems with power-law hopping,” *Phys. Rev. B* **96**, 054202 (2017).
- [33] X. Li, J. H. Pixley, D. L. Deng, S. Ganeshan, and S. Das Sarma, “Quantum nonergodicity and fermion localization in a system with a single-particle mobility edge,” *Phys. Rev. B* **93**, 184204 (2016).
- [34] X. Li, X. Li and S. Das Sarma, “Mobility edges in one-dimensional bichromatic incommensurate potentials,” *Phys. Rev. B* **96**, 085119 (2017).
- [35] L. Gong, Y. Feng, and Y. Ding, “Anderson localization in one-dimensional quasiperiodic lattice models with nearest- and next-nearest-neighbor hopping,” *Phys. Lett. A* **381**, 588 (2017).
- [36] H. P. Lüschen *et al.*, “Single-Particle Mobility Edge in a One-Dimensional Quasiperiodic Optical Lattice,” *Phys. Rev. Lett.* **120**, 160404 (2018).
- [37] F. A. An, E. J. Meier, and B. Gadway, “Engineering a Flux-Dependent Mobility Edge in Disordered Zigzag Chains,” *Phys. Rev. X* **8**, 031045 (2018).
- [38] D. R. Hofstadter, “Energy levels and wave functions of Bloch electrons in rational and irrational magnetic fields,” *Phys. Rev. B* **14**, 2239 (1976).
- [39] N. Goldman, A. Kubasiak, A. Bermudez, P. Gaspard, M. Lewenstein, and M. A. Martin-Delgado, “Non-Abelian Optical Lattices: Anomalous Quantum Hall Effect and Dirac Fermions,” *Phys. Rev. Lett.* **103**, 035301 (2009).
- [40] N. Goldman, A. Kubasiak, P. Gaspard, and M. Lewenstein, “Ultracold atomic gases in non-Abelian gauge potentials: The case of constant Wilson loop,” *Phys. Rev. A* **79**, 023624 (2009).
- [41] J. M. Hou, W. X. Yang, and X. J. Liu, “Massless Dirac fermions in a square optical lattice,” *Phys. Rev. A* **79**, 043621 (2009).
- [42] A. Bermudez *et al.*, “Wilson Fermions and Axion Electrodynamics in Optical Lattices,” *Phys. Rev. Lett.* **105**, 190404 (2010).
- [43] M. Kohmoto, “Metal-Insulator Transition and Scaling for Incommensurate Systems,” *Phys. Rev. Lett.* **51**, 1198 (1983).
- [44] H. Hiramoto and M. Kohmoto, “New Localization in a Quasiperiodic System,” *Phys. Rev. Lett.* **62**, 2714 (1989).
- [45] Jun Wang, Xia-Ji Liu, Gao Xianlong, and Hui Hu, “Phase diagram of a non-Abelian Aubry-André-Harper model with  $p$ -wave superfluidity,” *Phys. Rev. B* **93**, 104504 (2016).
- [46] I. Satija, D. Dakin, and C. Clark, “Metal-Insulator Transition Revisited for Cold Atoms in Non-Abelian Gauge Potentials,” *Phys. Rev. Lett.* **97**, 216401 (2006).